

Two-photon partial widths of tensor mesons

A.V. Anisovich, V.V. Anisovich, M.A. Matveev, and V.A. Nikonov

Abstract

We calculate partial widths of the $\gamma\gamma$ decay of the tensor $q\bar{q}$ states $a_2(1320)$, $f_2(1270)$, $f_2(1525)$, their radial excitations $a_2(1660)$, $f_2(1640)$, $f_2(1800)$ as well as ${}^3F_2q\bar{q}$ states. Calculations are performed in the framework of the same approach which was used before for the study of radiative decays $f_0(980) \rightarrow \gamma\gamma$, $a_0(980) \rightarrow \gamma\gamma$ and $\phi(1020) \rightarrow \gamma f_0(980)$: the assumption made is that of $q\bar{q}$ structure of $f_0(980)$ and $a_0(980)$ [A.V. Anisovich et al., Phys. Lett. B **456**, 80 (1999); Eur. Phys. J. A **12**, 103 (2001)]. The description of the decay partial widths for $a_2(1320)$, $f_2(1270)$, $f_2(1525)$ and $f_0(980)$, $a_0(980)$ is reached with the approximately equal radial wave functions, thus giving a strong argument in favour of the fact that these scalar and tensor mesons are to be classified as members of the same P -wave $q\bar{q}$ multiplet.

1 Introduction

For the time being the main problem of meson spectroscopy is the reliable determination of states belonging to the P -wave $q\bar{q}$ multiplet $1^3P_Jq\bar{q}$. The solution of this problem is of principal importance for the quark systematics

as well as for the search of exotic mesons such as glueballs and hybrids (in connection with this problem see [1-4]). The classification of mesons $f_0(980)$ and $a_0(980)$, that is of crucial meaning for the nonet of scalar mesons $1^3P_0q\bar{q}$, gives rise to certain questions. In a set of papers [5-10], on the basis of the analysis of experimental data, it was argued that for the states $f_0(980)$ and $a_0(980)$ the $1^3P_0q\bar{q}$ component is dominant. However, another point of view on the structure of these mesons exists as well, see mini-review [11] and references therein.

The investigation of radiative decays is a powerful tool for establishing the quark structure of hadrons. At early stage of the quark model, radiative decays of vector mesons provided strong evidence for constituent quark being a universal constructive element of mesons and baryons [12-15]. In our opinion, the radiative decays of the $1^3P_Jq\bar{q}$ mesons are equally important for the determination of the P -wave multiplet.

Partial widths of the decays $f_0(980) \rightarrow \gamma\gamma$ and $a_0(980) \rightarrow \gamma\gamma$ have been calculated in [9] assuming the mesons $f_0(980)$ and $a_0(980)$ to be dominantly $q\bar{q}$ states, that is, $1^3P_0q\bar{q}$ mesons. The results of our calculation agree well with experimental data. In paper [10], on the basis of data [16] for the decay $\phi(1020) \rightarrow \gamma f_0(980)$ together with the value of partial width $f_0(980) \rightarrow \gamma\gamma$ obtained in the re-analysis [17], the flavour content of $f_0(980)$ has been studied. Assuming the flavour wave function in the form $n\bar{n} \cos \varphi + s\bar{s} \sin \varphi$, we have described the experimental data with two allowed values of mixing angle: either $\varphi = -48^\circ \pm 6^\circ$ or $\varphi = 85^\circ \pm 4^\circ$ (the negative angle is more preferable). Both values of mixing angle are in qualitative agreement with data on hadronic decays of $f_0(980)$ into $\pi\pi$ and $K\bar{K}$ [8, 18].

Although direct calculations of widths of radiative decays agree well with the hypothesis that the $q\bar{q}$ component dominates both $f_0(980)$ and $a_0(980)$, to be confident that these mesons are members of $1^3P_0q\bar{q}$ multiplet one more step is necessary: it is necessary to check whether radiative decays of tensor mesons $a_2(1320)$, $f_2(1270)$, $f_2(1525)$ can be calculated under the same assumption and within the same technique as it was done for the reactions involving $f_0(980)$ and $a_0(980)$. The tensor mesons $a_2(1320)$, $f_2(1270)$, $f_2(1525)$ are basic members of the P -wave $q\bar{q}$ multiplet, and just the existence of tensor mesons lays in the ground of the nonet classification of mesons as $q\bar{q}$ -states, with four P -wave nonets [19, 20].

In the framework of spectral integration technique, we calculate the transition form factors of tensor mesons $a_2(1320) \rightarrow \gamma^*(Q^2)\gamma$, $f_2(1270) \rightarrow \gamma^*(Q^2)\gamma$ and $f_2(1525) \rightarrow \gamma^*(Q^2)\gamma$ in the region of small Q^2 : these form factors, in the limit $Q^2 \rightarrow 0$, determine partial widths $a_2(1320) \rightarrow \gamma\gamma$, $f_2(1270) \rightarrow \gamma\gamma$ and $f_2(1525) \rightarrow \gamma\gamma$. The spectral representation technique has been developed in [21] for the investigation of the transitions of pseudoscalar mesons such as $\pi^0 \rightarrow \gamma^*(Q^2)\gamma$, $\eta \rightarrow \gamma^*(Q^2)\gamma$ and $\eta' \rightarrow \gamma^*(Q^2)\gamma$. As is said above, by using this technique the calculation of the decay coupling constants $f_0(980) \rightarrow \gamma\gamma$, $a_0(980) \rightarrow \gamma\gamma$ and $\phi(1020) \rightarrow \gamma f_0(980)$ has been performed in [9, 10].

In the region of moderately small Q^2 , where Strong-QCD works, the transition form factor $q\bar{q}$ -meson $\rightarrow \gamma^*(Q^2)\gamma$ is determined by the quark loop diagram of Fig. 1a which is a convolution of the $q\bar{q}$ -meson and photon wave functions, $\Psi_{q\bar{q}} \otimes \Psi_\gamma$. The calculation of the process of Fig. 1a is performed in terms of the double spectral representation over $q\bar{q}$ invariant masses squared, $s = (m^2 + k_\perp^2)/(x(1-x))$ and $s' = (m^2 + k'_\perp^2)/(x(1-x))$ where k_\perp^2 , k'_\perp^2 and x are the light-cone variables and m is the constituent quark mass. Follow-

ing [21], we represent photon wave function as a sum of the two components which describe the prompt production of the $q\bar{q}$ pair at large s' (with a point-like vertex for the transition $\gamma \rightarrow q\bar{q}$, correspondingly) and the production in the low- s' region where the vertex $\gamma \rightarrow q\bar{q}$ has a nontrivial structure due to soft $q\bar{q}$ interactions. The necessity to include such a component can be argued, for example, by the vector-dominance model $\gamma \rightarrow \rho^0, \omega, \phi \rightarrow q\bar{q}$.

The process of Fig. 1a at moderately small Q^2 is mainly determined by the low- s' region, in other words by the soft component of photon wave function.

The soft component of the photon wave function was restored in [21], on the basis of the experimental data for the transition $\pi^0 \rightarrow \gamma^*(Q^2)\gamma$ at $Q^2 \leq 1$ GeV². Once the photon wave function is found, the form factors $a_2 \rightarrow \gamma^*(Q^2)\gamma$ and $f_2 \rightarrow \gamma^*(Q^2)\gamma$ at $Q^2 \leq 1$ GeV² provide us the opportunity to investigate in detail the tensor-meson wave functions. However, when investigating a small- Q^2 region, we may restrict ourselves with a simplified, one-parameter wave function of the basic tensor mesons $1^3P_2 q\bar{q}$, this parameter being the mean radius squared R_T^2 .

Assuming the $q\bar{q}$ structure of tensor mesons, the flavour content of $a_2(1320)$ is fixed, thus allowing unambiguous calculation of the transition form factor $a_2(1320) \rightarrow \gamma\gamma$. Reasonable agreement with data has been obtained at $7 \text{ GeV}^{-2} \leq R_{a_2(1320)}^2 \leq 12 \text{ GeV}^{-2}$ (remind that for pion $R_\pi^2 \simeq 10 \text{ GeV}^{-2} \simeq 0.4 \text{ fm}^2$). To describe the decay $a_0(980) \rightarrow \gamma\gamma$ the quark wave function of $a_0(980)$ should have nearly the same mean radius square [9] $7 \text{ GeV}^{-2} \leq R_{a_0(980)}^2 \leq 12 \text{ GeV}^{-2}$. Still, we do not exclude the possibility that the P -wave states may be rather compact. Hadronic reactions agree with this possibility: the estimation of radius of $f_0(980)$ carried out by using GAMS data for $\pi^- p \rightarrow \pi^0 \pi^0 n$

[22] proves that $q\bar{q}$ component in $f_0(980)$ gives [7]: $R_{f_0(980)}^2 = (6 \pm 6) \text{ GeV}^{-2}$.

Partial widths $\Gamma(f_2(1270) \rightarrow \gamma\gamma)$ and $\Gamma(f_2(1525) \rightarrow \gamma\gamma)$ depend on the relative weights of strange and non-strange components in a tensor-isoscalar meson, $s\bar{s}$ and $n\bar{n}$. The study of hadronic decays tells us that $f_2(1270)$ is dominantly $n\bar{n}$ state, while $f_2(1525)$ is, correspondingly, $s\bar{s}$ one. It is in accordance with the calculated values of partial widths $\Gamma(f_2(1270) \rightarrow \gamma\gamma)$ and $\Gamma(f_2(1525) \rightarrow \gamma\gamma)$: at $R_{f_2(1270)}^2 \simeq R_{f_2(1525)}^2 \sim R_{f_0(980)}^2$, the agreement with data is reached with $n\bar{n}$ - and $s\bar{s}$ -dominated components in $f_2(1270)$ and $f_2(1525)$, respectively.

The two-photon decays of radial-excited states, $2^3P_2q\bar{q} \rightarrow \gamma\gamma$, are suppressed as compared to decays of basic states. The reason is that radial wave functions of the states $2^3P_2q\bar{q}$ change sign, so the convolution of wave function $\psi_{2^3P_2q\bar{q}} \otimes \psi_\gamma$ is comparatively small. This fact is also the reason of a qualitative character of predictions for the decays $2^3P_2q\bar{q} \rightarrow \gamma\gamma$.

The paper is organized as follows. In Section 2 we present basic formulae for the calculation of amplitudes for $\gamma\gamma$ decaying into tensor mesons, members of the $1^3P_2q\bar{q}$ and $2^3P_2q\bar{q}$ nonets. The results of the calculation are given in Section 3. In Conclusion we discuss the $q\bar{q}$ multiplet classification of tensor and scalar mesons resulting from radiative meson decays.

2 Tensor-meson decay amplitudes for the process $q\bar{q} (2^{++}) \rightarrow \gamma\gamma$

Below the formulae are presented for the amplitudes of radiative decay of the $q\bar{q}$ tensor mesons belonging to the multiplets located at $\lesssim 2000$ MeV: $1^3P_2q\bar{q}$, $2^3P_2q\bar{q}$ and $1^3F_2q\bar{q}$.

2.1 Spin-momentum structure of the decay amplitude

The decay amplitude for the process $q\bar{q} (2^{++}) \rightarrow \gamma\gamma$ has the following structure:

$$A_{\mu\nu,\alpha\beta}^{(T)} = e^2 \left[S_{\mu\nu,\alpha\beta}^{(0)}(p, q) F_{T \rightarrow \gamma\gamma}^{(0)}(0, 0) + S_{\mu\nu,\alpha\beta}^{(2)}(p, q) F_{T \rightarrow \gamma\gamma}^{(2)}(0, 0) \right], \quad (1)$$

where e is the electron charge ($e^2/4\pi = \alpha = 1/137$). Here $S_{\mu\nu,\alpha\beta}^{(0)}$ and $S_{\mu\nu,\alpha\beta}^{(2)}$ are the moment-operators, indices α, β refer to photons and μ, ν to tensor meson. The transition form factors for photons with transverse polarization $T \rightarrow \gamma_\perp(q_1^2)\gamma_\perp(q_2^2)$, namely, $F_{T \rightarrow \gamma\gamma}^{(0)}(q_1^2, q_2^2)$ and $F_{T \rightarrow \gamma\gamma}^{(2)}(q_1^2, q_2^2)$, depend on the photon momenta squared q_1^2 and q_2^2 ; the limit values $q_1^2 = 0$ and $q_2^2 = 0$ correspond to the two-photon decay. We also use the notations: $p = q_1 + q_2$ and $q = (q_1 - q_2)/2$.

The moment-operators read:

$$S_{\mu\nu,\alpha\beta}^{(0)}(p, q) = g_{\alpha\beta}^{\perp\perp} \left(\frac{q_\mu q_\nu}{q^2} - \frac{1}{3} g_{\mu\nu}^{\perp\perp} \right) \quad (2)$$

and

$$S_{\alpha\beta, \mu\nu}^{(2)}(p, q) = g_{\mu\alpha}^{\perp\perp} g_{\nu\beta}^{\perp\perp} + g_{\mu\beta}^{\perp\perp} g_{\nu\alpha}^{\perp\perp} - g_{\mu\nu}^{\perp\perp} g_{\alpha\beta}^{\perp\perp}, \quad (3)$$

where metric tensors $g_{\mu\nu}^{\perp}$ and $g_{\alpha\beta}^{\perp\perp}$ are determined as follows:

$$g_{\mu\nu}^{\perp} = g_{\mu\nu} - \frac{p_\mu p_\nu}{p^2}, \quad g_{\alpha\beta}^{\perp\perp} = g_{\alpha\beta} - \frac{q_\alpha q_\beta}{q^2} - \frac{p_\alpha p_\beta}{p^2}. \quad (4)$$

The moment-operators are orthogonal in the space of photon polarizations:

$$S_{\mu\nu,\alpha\beta}^{(0)} S_{\mu'\nu',\alpha\beta}^{(2)} = 0.$$

The spin structure of the amplitude $A_{\mu\nu,\alpha\beta}^{(T)}$ is discussed in more detail in Appendix A, also there is presented a connection between amplitudes written in terms of spin operators and standard helicity amplitudes.

2.2 Form factor $F_{T \rightarrow \gamma\gamma}^{(H)}(q_1^2, q_2^2)$

Following the prescription of [21], we write down the amplitude of the process of Fig. 1a in terms of the spectral representation in the channels related to tensor meson and photon $\gamma(q_2)$. The double spectral representation for the form factor $F_{T \rightarrow \gamma\gamma}^{(H)}(q_1^2, q_2^2)$ with $H = 0, 2$ reads:

$$F_{T \rightarrow \gamma\gamma}^{(H)}(q_1^2, q_2^2) = Z_T \sqrt{N_c} \int_{4m^2}^{\infty} \frac{ds ds'}{\pi^2} \frac{G_{T \rightarrow q\bar{q}}(s)}{s - m_T^2} \times \quad (5)$$

$$\times d\Phi(P, P'; k_1, k'_1, k_2) S^{(H)}(P^2, P'^2, \tilde{q}^2) \frac{G_{\gamma \rightarrow q\bar{q}}(s')}{s' - q_2^2}.$$

In the spectral integral (5), the momenta of the intermediate states differ from those of the initial/final states. The corresponding momenta for intermediate states are re-denoted as is shown in Fig. 1b:

$$q_1 \rightarrow P - P', \quad q_2 \rightarrow P', \quad p \rightarrow P, \quad (6)$$

$$P^2 = s, \quad P'^2 = s', \quad (P' - P)^2 = \tilde{q}^2 = q_1^2.$$

It should be stressed that we fix $\tilde{q}^2 = q_1^2$, although $P' - P = \tilde{q} \neq q_1$. The triangle-diagram phase space $d\Phi(P, P'; k_1, k'_1, k_2)$ is equal to:

$$d\Phi(P, P'; k_1, k'_1, k_2) = \frac{1}{4} \frac{d^3 k_1}{(2\pi)^3 2k_{10}} \frac{d^3 k'_1}{(2\pi)^3 2k'_{10}} \frac{d^3 k_2}{(2\pi)^3 2k_{20}} \times \quad (7)$$

$$\times (2\pi)^4 \delta^{(4)}(P - k_1 - k_2) (2\pi)^4 \delta^{(4)}(P' - k'_1 - k_2).$$

The factor Z_T is determined by the quark content of tensor meson. For the a_2 -meson and $n\bar{n}$ or $s\bar{s}$ components in the f_2 -meson, the charge factors are equal to

$$Z_{a_2} = 2 \frac{e_u^2 - e_d^2}{\sqrt{2}}, \quad Z_{n\bar{n}} = 2 \frac{e_u^2 + e_d^2}{\sqrt{2}}, \quad Z_{s\bar{s}} = 2e_s^2. \quad (8)$$

The factor $\sqrt{N_c}$, where $N_c = 3$ is the number of colours, is related to the normalization of the photon vertex made in [21]. We have two sorts of diagrams: with quark lines drawn clockwise and anticlockwise; the factor 2 in (8) stands for this doubling. The vertices $G_{\gamma \rightarrow n\bar{n}}(s')$ and $G_{\gamma \rightarrow s\bar{s}}(s')$ were found in [21]; the photon wave function $G_{\gamma \rightarrow n\bar{n}}(s)/s$ is shown in Fig. 2.

2.2.1 Wave functions for the $1^3P_2q\bar{q}$ and $2^3P_2q\bar{q}$ states

We parametrize the wave functions of mesons of the basic multiplet, $1^3P_2q\bar{q}$, in the exponential form:

$$\Psi_T(s) = \frac{G_T(s)}{s - m_T^2} = C e^{-bs}, \quad (9)$$

where C is the normalization constant, $\Psi_T \otimes \Psi_T = 1$, and the parameter b can be related to the tensor-meson radius squared.

For mesons of the first radial excitation, $2^3P_2q\bar{q}$, the wave functions can be written using exponential approximation as

$$\Psi_{T_1}(s) = C_1 e^{-b_1 s} (D_1 s - 1). \quad (10)$$

The parameter b_1 can be related to the radius of the radial excitation state, then the values C_1 and D_1 are fixed by the normalization and orthogonality requirements, $\Psi_{T_1} \otimes \Psi_{T_1} = 1$ and $\Psi_T \otimes \Psi_{T_1} = 0$.

2.3 Spin structure factors $S^{(0)}(P^2, P'^2, \tilde{q}^2)$ and $S^{(2)}(P^2, P'^2, \tilde{q}^2)$

For the amplitude of Fig. 1b with transverse polarized photons, the spin structure factors are fixed by the vertex for transition $T \rightarrow q\bar{q}$, and we denote this vertex as $T_{\mu\nu}$. One has:

$$\begin{aligned} & \text{Tr} \left[\gamma_{\beta}^{\perp\perp} (\hat{k}'_1 + m) \gamma_{\alpha}^{\perp\perp} (\hat{k}_1 + m) T_{\mu\nu} (\hat{k}_2 - m) \right] = \\ & = S_{\mu\nu, \alpha\beta}^{(0)}(P, P'_{\perp}) S^{(0)}(P^2, P'^2, \tilde{q}^2) + S_{\mu\nu, \alpha\beta}^{(2)}(P, P'_{\perp}) S^{(2)}(P^2, P'^2, \tilde{q}^2) \end{aligned} \quad (11)$$

Here $\gamma_{\alpha}^{\perp\perp}$ and $\gamma_{\beta}^{\perp\perp}$ stand for photon vertices, $\gamma_{\alpha}^{\perp\perp} = g_{\alpha\alpha'}^{\perp\perp} \gamma_{\alpha'}$, while $g_{\alpha\alpha'}^{\perp\perp}$ is determined by (4) with the substitution $q_1 \rightarrow P - P'$ and $q_2 \rightarrow P'$. The momentum operators $S_{\mu\nu, \alpha\beta}^{(0)}(P, P'_{\perp})$ and $S_{\mu\nu, \alpha\beta}^{(2)}(P, P'_{\perp})$ work also in the intermediate-state momentum space. Recall that the momenta k'_1 , k_1 and k_2 in (11) are mass-on-shell.

The vertex $T_{\mu\nu}$ taken in a minimal form reads:

$$T_{\mu\nu}^{(k)} = k_{\mu} \gamma_{\nu} + k_{\nu} \gamma_{\mu} - \frac{2}{3} g_{\mu\nu}^{\perp} \hat{k}, \quad (12)$$

where $k = k_1 - k_2$ and $g_{\mu\nu}^{\perp} P_{\nu} = 0$. With $T_{\mu\nu}$ determined by (12), we present the spin structure factors $S^{(H)}(P^2, P'^2, \tilde{q}^2)$ at $q_2^2 = 0$ and small $q_1^2 = \tilde{q}^2 \equiv -Q^2$. Below we denote $\Sigma = (s + s')/2$ and $\Delta = s - s'$ and take into account that $\Delta \sim Q$. For the non-vanishing terms in the limit $Q^2 \rightarrow 0$, we have:

$$\begin{aligned} S^{(0)}(P^2, P'^2, -Q^2) &= \frac{64m^2 \Sigma^2 Q^4}{(\Delta^2 + 4\Sigma Q^2)^2} (4m^2 - \Sigma) + \\ &+ \frac{4\Sigma Q^2 \Delta^2}{(\Delta^2 + 4\Sigma Q^2)^2} (32m^4 + 8m^2 \Sigma - 3\Sigma^2) + \frac{4m^2 \Delta^4}{(\Delta^2 + 4\Sigma Q^2)^2} (4m^2 + 3\Sigma) \end{aligned} \quad (13)$$

and

$$S^{(2)}(P^2, P'^2, -Q^2) = \frac{8\Sigma^2 Q^4}{(\Delta^2 + 4\Sigma Q^2)^2} (-16m^4 + \Sigma^2) + \quad (14)$$

$$+ \frac{4\Sigma Q^2 \Delta^2}{(\Delta^2 + 4\Sigma Q^2)^2} \left(-16m^4 - 4m^2\Sigma + \Sigma^2 \right) + \frac{4m^2 \Delta^4}{(\Delta^2 + 4\Sigma Q^2)^2} \left(-2m^2 - \Sigma \right).$$

2.3.1 Spin structure factors $S^{(H)}(P^2, P'^2, \tilde{q}^2)$ for pure $q\bar{q}$ ($L = 1$) and $q\bar{q}$ ($L = 3$) states

The $q\bar{q}$ (2^{++}) state can be constructed in two ways, namely, with the $q\bar{q}$ orbital momenta $L = 1$ and $L = 3$ (the ${}^3P_2 q\bar{q}$ and ${}^3F_2 q\bar{q}$ states). The vertex $T_{\mu\nu}$ of Eq. (12), corresponding to the dominant P -wave $q\bar{q}$ state, includes also certain admixture of the F -wave $q\bar{q}$ state.

The vertex for the production of pure $q\bar{q}$ ($L = 1$) state reads:

$$T_{\mu\nu}^{(L=1),(k)} = k_\mu \Gamma_\nu + k_\nu \Gamma_\mu - \frac{2}{3} g_{\mu\nu}^\perp(\Gamma k), \quad \Gamma_\mu = \gamma_\mu^\perp - \frac{k_\mu}{2m + \sqrt{s}}, \quad (15)$$

where the operator Γ_μ selects the spin-1 state for $q\bar{q}$ (see [23, 24] for details).

We present corresponding spin factors, $S_{L=1}^{(0)}(P^2, P'^2, -Q^2)$ and $S_{L=1}^{(2)}(P^2, P'^2, -Q^2)$, in Appendix B.

The ($L = 3$)-operator for the ${}^3F_2 q\bar{q}$ state is equal to:

$$T_{\mu\nu}^{(L=3),(k)} = k_\mu k_\nu (\Gamma k) - \frac{k^2}{5} \left(g_{\mu\nu}^\perp(\Gamma k) + \Gamma_\mu k_\nu + \Gamma_\nu k_\mu \right). \quad (16)$$

Corresponding spin factors, $S_{L=3}^{(0)}(P^2, P'^2, -Q^2)$ and $S_{L=3}^{(2)}(P^2, P'^2, -Q^2)$, are also given in Appendix B.

2.4 Spectral integral representation

In formula (5) one can integrate over the phase space by using δ -functions, with fixed the energies squared, s and s' . So we have:

$$F_{T \rightarrow \gamma\gamma}^{(H)}(-Q^2, 0) = \quad (17)$$

$$= Z_T \sqrt{N_c} \int_{4m^2}^{\infty} \frac{ds ds'}{\pi^2} \psi_T(s) \psi_\gamma(s') \frac{\theta(ss'Q^2 - m^2 \lambda(s, s', -Q^2))}{16\sqrt{\lambda(s, s', -Q^2)}} S_{T \rightarrow \gamma\gamma}^{(H)}(s, s', -Q^2),$$

with

$$\lambda(s, s', -Q^2) = (s' - s)^2 + 2Q^2(s' + s) + Q^4. \quad (18)$$

The θ -function restricts the integration region for different Q^2 : $\theta(X) = 1$ at $X \geq 0$ and $\theta(X) = 0$ at $X < 0$.

In the limit $Q^2 \rightarrow 0$, one has

$$F_{T \rightarrow \gamma\gamma}^{(H)}(-Q^2 \rightarrow 0, 0) = Z_T \sqrt{N_c} \int_{4m^2}^{\infty} \frac{d\Sigma}{\pi} \psi_T(\Sigma) \psi_\gamma(\Sigma) \int_{-b}^{+b} \frac{d\Delta}{\pi} \frac{S_{T \rightarrow \gamma\gamma}^{(H)}(s, s', -Q^2)}{16\sqrt{\Lambda(\Sigma, \Delta, Q^2)}}$$

$$b = Q\sqrt{\Sigma(\Sigma/m^2 - 4)}, \quad \Lambda(\Sigma, \Delta, Q^2) = \Delta^2 + 4\Sigma Q^2. \quad (19)$$

Where the spin factors $S_{T \rightarrow \gamma\gamma}^{(H)}(s, s', -Q^2)$ are given in (13) and (14).

The integration over Δ performed, the spectral representation for the form factor $F_{T \rightarrow \gamma\gamma}^{(H)}(0, 0)$ reads:

$$F_{T \rightarrow \gamma\gamma}^{(H)}(0, 0) = \frac{Z_T^{(q\bar{q})} \sqrt{N_c}}{16\pi} \int_{4m^2}^{\infty} \frac{ds}{\pi} \psi_T(s) \psi_\gamma(s) I^{(H)}(s) \quad (20)$$

where

$$I^{(0)}(s) = -2\sqrt{s(s-4m^2)} (12m^2 + s) + 4m^2 (4m^2 + 3s) \ln \frac{s + \sqrt{s(s-4m^2)}}{s - \sqrt{s(s-4m^2)}} \quad (21)$$

and

$$I^{(2)}(s) = \frac{4\sqrt{s(s-4m^2)}}{3} (5m^2 + s) - 4m^2 (2m^2 + s) \ln \frac{s + \sqrt{s(s-4m^2)}}{s - \sqrt{s(s-4m^2)}} \quad (22)$$

The tensor-meson decay form factors $T \rightarrow \gamma\gamma$ with vertices $T \rightarrow q\bar{q}$ for pure $q\bar{q}$ ($L = 1$) and $q\bar{q}$ ($L = 3$) states (see (15) and (16)) are given in Appendix C.

2.5 Light-cone variables

The formula (5) allows one to make easily the transformation to the light-cone variables using the boost along the z -axis. Let us use the frame in which initial tensor meson is moving along the z -axis with the momentum $p \rightarrow \infty$:

$$P = (p + \frac{s}{2p}, 0, p), \quad P' = (p + \frac{s' + Q^2}{2p}, \mathbf{Q}, \mathbf{p}). \quad (23)$$

Then the transition form factor $T \rightarrow \gamma^*(Q^2)\gamma$ reads:

$$F_{T \rightarrow \gamma\gamma}^{(H)}(-Q^2, 0) = \frac{Z_T \sqrt{N_c}}{16\pi^3} \int_0^1 \frac{dx}{x(1-x)^2} \int d^2k_\perp \Psi_T(s) \Psi_\gamma(s') S^{(H)}(s, s', -Q^2), \quad (24)$$

where $x = k_{2z}/p$, $\mathbf{k}_\perp = \mathbf{k}_{2\perp}$, and the $q\bar{q}$ invariant mass squares are

$$s = \frac{m^2 + k_\perp^2}{x(1-x)}, \quad s' = \frac{m^2 + (-x\mathbf{Q} + \mathbf{k}_\perp)^2}{x(1-x)}. \quad (25)$$

2.6 Tensor-meson charge form factor

In order to relate the wave function parameters C and b entering (9) to the tensor-meson radius squared, we calculate the meson charge form factor averaged over polarizations; corresponding process is shown diagrammatically in Fig. 1c. Thus determined form factor amplitude has the structure as follows:

$$A_\mu = (p_\mu + p'_\mu) F_T(-Q^2), \quad (26)$$

where the meson charge form factor $F_T(Q^2)$ is the convolution of the tensor-meson wave functions $\Psi_T \otimes \Psi_T$.

2.6.1 Charge form factor in the light-cone variables

Using light-cone variables, one can express the $q\bar{q}$ -meson charge form factor as follows (for example, see [10, 21]):

$$F_T(-Q^2) = \frac{1}{16\pi^3} \int_0^1 \frac{dx}{x(1-x)^2} \int d^2k_\perp \Psi_T(s) \Psi_T(s') S_T(s, s', -Q^2), \quad (27)$$

$S_T(s, s', -Q^2)$ being determined by the quark loop trace in the intermediate state:

$$\begin{aligned} & \frac{1}{5} \text{Tr}[\Gamma_{\mu\nu}^{(k)}(\hat{k}_1 + m) \gamma_\alpha(\hat{k}'_1 + m) \Gamma_{\mu\nu}^{(k')}(\hat{k}_2 - m)] = \\ & = [P'_\alpha + P_\alpha - \frac{s' - s}{Q^2}(P'_\alpha - P_\alpha)] S_T(s, s', -Q^2), \end{aligned} \quad (28)$$

where $(P' - P)^2 = -Q^2$.

To relate the wave function parameters to the tensor-meson radius squared we may restrict ourselves by the consideration of the low- Q^2 region. The low- Q^2 charge form factor can be expanded in a series over Q^2 :

$$F_T(-Q^2) \simeq 1 - \frac{1}{6} R_T^2 Q^2. \quad (29)$$

At small Q^2 one has for $S_T(s, s', -Q^2)$:

$$\begin{aligned} S_T(s, s', -Q^2) = & \frac{Q^2}{45(\Delta^2 + 4\Sigma Q^2)\Sigma^2} \left[-48\Sigma^3(8m^2 + 3\Sigma)(4m^2 - \Sigma) - \right. \\ & \left. -16Q^2\Sigma^2(64m^4 - 22m^2\Sigma + 9\Sigma^2) + 8\Sigma\Delta^2(40m^4 + 29m^2\Sigma - 9\Sigma^2) \right] - \\ & - \frac{Q^2\Sigma^3(8m^2 + 3\Sigma)(4m^2 - \Sigma)}{45(\Delta^2 + 4\Sigma Q^2)^2} \left[\frac{\Delta^4}{4\Sigma^4} + \frac{Q^2\Delta^2}{\Sigma^3} - \frac{Q^4}{\Sigma^2} \right]. \end{aligned} \quad (30)$$

Recall, $\Sigma = (s + s')/2$ and $\Delta = s - s'$.

2.6.2 Spectral integral representation for charge form factor

Expanded in a series over Q^2 , the spectral integral for charge form factor, $F_T(-Q^2)$, reads:

$$F_T(-Q^2) \simeq \frac{1}{16\pi} \int_{4m^2}^{\infty} \frac{ds}{\pi} \psi_T^2(s) \left(I(s) - \frac{Q^2}{6} I_R(s) \right), \quad (31)$$

where

$$\begin{aligned} I(s) &= \frac{8\sqrt{s(s-4m^2)}}{15s} (8m^2 + 3s) (s - 4m^2), \\ I_R(s) &= \frac{4\sqrt{s(s-4m^2)}}{5s^3} (-64m^6 - 40m^4s + 26m^2s^2 + 9s^3) + \\ &+ \frac{8}{15s} (16m^4 - 46m^2s + 9s^2) \ln \frac{s + \sqrt{s(s-4m^2)}}{s - \sqrt{s(s-4m^2)}}. \end{aligned} \quad (32)$$

Comparison of this expression with formula (29) gives us the parameters of the tensor-meson wave function.

Formulae (31) and (32) can be used for the determination of the wave function parameters for any $n^3P_2q\bar{q}$ meson.

3 Results

Here are presented the results of the calculation of the $\gamma\gamma$ partial widths for mesons of the basic multiplet $1^3P_2q\bar{q}$, that is, $a_2(1320)$, $f_2(1270)$ and $f_2(1525)$. According to [25], mesons of the first radial excitation, $2^3P_2q\bar{q}$, are $a_2(1660)$, $f_2(1640)$ and $f_2(1800)$, and we calculate their $\gamma\gamma$ partial widths as well. We estimate also the $\gamma\gamma$ widths of the F -wave mesons, namely, the members of $1^3F_2q\bar{q}$ nonet, these mesons are located in the vicinity of 2000 MeV [25].

3.1 Tensor-meson $\gamma\gamma$ decay partial width

Partial width, $\Gamma_{T\rightarrow\gamma\gamma}$, is determined as follows:

$$\begin{aligned} m_T \Gamma_{T\rightarrow\gamma\gamma} &= \frac{1}{2} \int d\Phi_2(p; q_1, q_2) \frac{1}{5} \sum_{\mu\nu, \alpha\beta} |A_{\mu\nu, \alpha\beta}|^2 = \\ &= \frac{4}{5} \pi \alpha^2 \left[\frac{1}{3} \left(F_{T\rightarrow\gamma\gamma}^{(0)}(0, 0) \right)^2 + \left(F_{T\rightarrow\gamma\gamma}^{(2)}(0, 0) \right)^2 \right]. \end{aligned} \quad (33)$$

Here m_T is the mass of the tensor meson; the summation is carried out over outgoing-photon polarizations; the photon identity factor 1/2 is written explicitly; averaging over the tensor-meson polarizations results in the factor 1/5. The two-particle invariant phase space is equal to

$$d\Phi_2(p; q_1, q_2) = \frac{1}{2} \frac{d^3 q_1}{(2\pi)^3 2q_{10}} \frac{d^3 q_2}{(2\pi)^3 2q_{20}} (2\pi)^4 \delta^{(4)}(p - q_1 - q_2), \quad (34)$$

and for photons $\int d\Phi_2(p; q_1, q_2) = 1/16\pi$.

3.2 Transition form factors $F_{n\bar{n}\rightarrow\gamma\gamma}^{(H)}$ and $F_{s\bar{s}\rightarrow\gamma\gamma}^{(H)}$ for mesons of the $1^3P_2 q\bar{q}$ nonet

The transition form factors $F_{n\bar{n}\rightarrow\gamma\gamma}^{(H)}$ and $F_{s\bar{s}\rightarrow\gamma\gamma}^{(H)}$ are determined by Eq. (20). They depend on the quark mass and type of the vertex entering the spin factor, as well as the tensor meson wave function. For non-strange quarks, the ratios $F_{a_2\rightarrow\gamma\gamma}^{(H)}(0, 0)/Z_{a_2}$ and $F_{n\bar{n}\rightarrow\gamma\gamma}^{(H)}(0, 0)/Z_{n\bar{n}}$ are equal to one another, provided a_2 and $(n\bar{n})_2$ -state belong to the same $q\bar{q}$ multiplet. The magnitudes $F_{n\bar{n}\rightarrow\gamma\gamma}^{(H)}(0, 0)$ and $F_{s\bar{s}\rightarrow\gamma\gamma}^{(H)}(0, 0)$ are shown in Fig. 3 for different tensor mesons.

The transition form factors for mesons of the basic multiplet $1^3P_2 q\bar{q}$ for the case when the transition vertex $T \rightarrow q\bar{q}$ is chosen in the minimal form (12) are shown in Fig. 3a. Form factors decrease noticeably with the increase of radius

of the $q\bar{q}$ system in the interval $6 \text{ GeV}^{-2} \leq R_T^2 \leq 16 \text{ GeV}^{-2}$. The calculated form factors reveal a strong dependence on the quark mass. In our calculations we put $m = 350 \text{ MeV}$ for the non-strange quark and $m = 500 \text{ MeV}$ for the strange one. One can see that with the increase of quark mass by 150 MeV the transition form factors fall down, with a factor 1.5.

In Fig. 3b the form factors $F_{q\bar{q} \rightarrow \gamma\gamma}^{(H)}(0,0)/Z_{q\bar{q}}$ are shown for mesons $1^3P_2 q\bar{q}$ in case when the vertex $T \rightarrow q\bar{q}$ is taken in the form (15), that corresponds to a pure P -wave.

3.3 Decays $a_2 \rightarrow \gamma\gamma$

The form factor $F_{a_2 \rightarrow \gamma\gamma}^{(H)}(0,0)$ is equal to that of the $n\bar{n}$ component, up to the charge factor:

$$F_{a_2 \rightarrow \gamma\gamma}^{(H)}(0,0) = \frac{Z_{a_2}}{Z_{n\bar{n}}} F_{n\bar{n} \rightarrow \gamma\gamma}^{(H)}(0,0) . \quad (35)$$

Since flavour structure of the a_2 -meson is fixed, we can calculate partial $\gamma\gamma$ widths rather reliably.

In Fig. 4 the magnitudes of $\Gamma_{a_2(1320) \rightarrow \gamma\gamma}$ are shown versus $R_{a_2(1320)}^2$ together with experimental data.

Recent measurements of the $\gamma\gamma$ partial width of the $a_2(1320)$ -meson reported the magnitudes $\Gamma_{a_2(1320) \rightarrow \gamma\gamma} = 0.98 \pm 0.05 \pm 0.09 \text{ keV}$ [26] and $\Gamma_{a_2(1320) \rightarrow \gamma\gamma} = 0.96 \pm 0.03 \pm 0.13 \text{ keV}$ [27] (corresponding areas are shown by close hatched lines in Fig. 4). Besides, one should take into consideration that the extraction of the signal $a_2(1320) \rightarrow \gamma\gamma$ faces the problem of a correct account for coherent background. In the analysis [28] it was shown that the measured value of $\Gamma_{a_2(1320) \rightarrow \gamma\gamma}$ can fall down in a factor ~ 1.5 due to the interference "signal-

background". Therefore, we estimate the allowed region for $\Gamma_{a_2(1320) \rightarrow \gamma\gamma}$ as $1.12 \text{ keV} \leq \Gamma_{a_2(1320) \rightarrow \gamma\gamma} \leq 0.60 \text{ keV}$ (rare hatched lines in Fig. 4).

Figure 5a demonstrates a full set of the $a_2 \rightarrow \gamma\gamma$ widths. Thick solid line is drawn for $\Gamma(a_2(1320) \rightarrow \gamma\gamma)$ with the vertex given by (9) and (12) while the dashed line presents $\Gamma(a_2(1320) \rightarrow \gamma\gamma)$ for the vertex given by (9) and (15). The thin solid and dotted lines show correspondingly $\Gamma(a_2(1660) \rightarrow \gamma\gamma)$ for the vertex given by (10) and (12) and $\Gamma(a_2(\sim 2000) \rightarrow \gamma\gamma)$ for the vertex given by (9) and (16).

When comparing the calculated values with experimental data, one should keep in mind that quark masses are strictly fixed: as was mentioned above, $m = 350 \text{ MeV}$ for the non-strange quark and $m = 500 \text{ MeV}$ for strange one. The same mass values have been used in [10] for the calculation of the decays $a_0(980) \rightarrow \gamma\gamma$ and $f_0(980) \rightarrow \gamma\gamma$. Still, the two-photon decays of scalar mesons depend comparatively weakly on quark masses, while for tensor meson the situation is quite opposite: the decrease of constituent quark mass by 10% results in the increase of the form factor $F_{n\bar{n}}^{(H)}(0, 0)$ approximately by 10%, that means a 20% growth of the calculated value of $\Gamma_{a_2(1320) \rightarrow \gamma\gamma}$ at fixed $R_{a_2(1320)}^2$. The 10%-uncertainty in the definition of the constituent quark mass looks quite reasonable, therefore the 20% accuracy of the model prediction for $\Gamma_{a_2(1320) \rightarrow \gamma\gamma}$ should be regarded as quite normal.

Coming back to the decay $a_2(1320) \rightarrow \gamma\gamma$ we conclude that calculated values $\Gamma_{a_2(1320) \rightarrow \gamma\gamma}$ demonstrate rather good agreement with data at $R_{a_2(1320)}^2 \lesssim 12 \text{ GeV}^{-2}$.

3.4 Decays $f_2(1270) \rightarrow \gamma\gamma$ and $f_2(1525) \rightarrow \gamma\gamma$

First, consider the decays of mesons belonging to basic $1^3P_2q\bar{q}$ nonet. We define flavour wave functions of $f_2(1270)$ and $f_2(1525)$ as follows:

$$\begin{aligned} f_2(1270) : & \quad \cos \varphi_T n\bar{n} + \sin \varphi_T s\bar{s} , \\ f_2(1525) : & \quad -\sin \varphi_T n\bar{n} + \cos \varphi_T s\bar{s} . \end{aligned} \quad (36)$$

Then the form factors of the two-photon decays of f_2 -mesons read:

$$\begin{aligned} F_{f_2(1270) \rightarrow \gamma\gamma}^{(H)}(0,0) &= \cos \varphi_T F_{n\bar{n} \rightarrow \gamma\gamma}^{(H)}(0,0) + \sin \varphi_T F_{s\bar{s} \rightarrow \gamma\gamma}^{(H)}(0,0), \\ F_{f_2(1525) \rightarrow \gamma\gamma}^{(H)}(0,0) &= -\sin \varphi_T F_{n\bar{n} \rightarrow \gamma\gamma}^{(H)}(0,0) + \cos \varphi_T F_{s\bar{s} \rightarrow \gamma\gamma}^{(H)}(0,0) . \end{aligned} \quad (37)$$

Hadronic decays tell us that $f_2(1270)$ is mainly $n\bar{n}$ system while $f_2(1525)$ is $s\bar{s}$, that is, the mixing angle φ_T is small.

Following [26-29] we accept partial widths as follows: $\Gamma_{f_2(1270) \rightarrow \gamma\gamma} = (2.60 \pm 0.25_{-0.25}^{+0.00})$ keV and $\Gamma_{f_2(1525) \rightarrow \gamma\gamma} = 0.097 \pm 0.015_{-0.25}^{+0.00}$ keV. The magnitude of the extracted signal depends on the type of a model used for the description of the background. For the coherent background the magnitude of the signal decreases, and the second error in $\Gamma_{f_2(1270) \rightarrow \gamma\gamma}$ and $\Gamma_{f_2(1525) \rightarrow \gamma\gamma}$ is related to the background uncertainties.

Figure 5b shows the values of $\Gamma_{f_2(1270) \rightarrow \gamma\gamma}$ and $\Gamma_{f_2(1525) \rightarrow \gamma\gamma}$ calculated under the assumption that $\varphi_T = 0$.

In Fig. 6 the results of the fit to data for $\Gamma_{f_2(1270) \rightarrow \gamma\gamma}$ and $\Gamma_{f_2(1525) \rightarrow \gamma\gamma}$ are shown, without any fixation of φ_T . One can see that there exist two solutions: $\varphi_T \simeq 0^\circ$ and $\varphi_T \simeq 25^\circ$, in both cases $R_T^2 \lesssim 10 \text{ GeV}^{-2}$. The rare hatched areas correspond to the description of data near the low border: $2.10 \text{ keV} \leq \Gamma_{f_2(1270) \rightarrow \gamma\gamma} \leq 2.35 \text{ keV}$ and $0.57 \text{ keV} \leq \Gamma_{f_2(1525) \rightarrow \gamma\gamma} \leq 0.82 \text{ keV}$.

3.5 Two-photon decays of the $2^3P_2q\bar{q}$ and $1^3F_2q\bar{q}$ states

As it follows from [25], at 1600–1800 MeV there are two tensor-isoscalar states – members of the $2^3P_2q\bar{q}$ multiplet: they are $f_2(1640)$ and $f_2(1800)$ (presumably $n\bar{n}$ - and $s\bar{s}$ -dominant states, correspondingly).

In Fig. 3c the form factors of mesons from radial excitation nonet $2^3P_2q\bar{q}$ are shown: the transition vertex $T \rightarrow q\bar{q}$ is defined by the wave function (10) and spin matrix (12). A small magnitude of transition form factors at $R_T^2 \gtrsim 10$ GeV⁻² is due to zero in the wave function (10). The form factor magnitudes calculated for the transitions $2^3P_2q\bar{q} \rightarrow \gamma\gamma$ are in some way approximate only – they strongly depend on the details of the wave functions of $2^3P_2q\bar{q}$ -states, and comparatively weak variation which, for example, does not change the mean radius square R^2 may affect the form factor value by 100%.

Special feature of the two-photon decays of radial-excitation mesons is that their partial widths are considerable smaller than corresponding widths of the basic mesons:

$$\begin{aligned} \Gamma_{1^3P_2n\bar{n} \rightarrow \gamma\gamma} &\gg \Gamma_{2^3P_2n\bar{n} \rightarrow \gamma\gamma} , \\ \Gamma_{1^3P_2s\bar{s} \rightarrow \gamma\gamma} &\gg \Gamma_{2^3P_2s\bar{s} \rightarrow \gamma\gamma} . \end{aligned} \quad (38)$$

The inequalities are due to the fact that radial wave function of $2^3P_2q\bar{q}$ -state contains a zero, therefore the convolution of wave functions $\psi_{2^3P_2q\bar{q}} \otimes \psi_\gamma$ is significantly smaller than the convolution $\psi_{1^3P_2q\bar{q}} \otimes \psi_\gamma$ (wave function of basic state has no zeros).

In Fig. 5c one can see partial widths for $f_2(1640) \rightarrow \gamma\gamma$ and $f_2(1800) \rightarrow \gamma\gamma$ calculated under simple hypothesis that $f_2(1640)$ is a pure $n\bar{n}$ state, while $f_2(1800)$ is pure $s\bar{s}$ state. One should emphasize that the probability for the

transition $2^3P_2n\bar{n} \rightarrow \gamma\gamma$ is higher by an order of value than $2^3P_2s\bar{s} \rightarrow \gamma\gamma$. This means that a comparatively small admixture of the $n\bar{n}$ component may considerably enhance the width of $\Gamma_{f_2(1800)\rightarrow\gamma\gamma}$, by a factor 2–3 as compared to what follows from pure $s\bar{s}$ state.

The verification of Eq. (38) is of principal meaning from the point of view of meson quark structure. Preliminary data of the L3 collaboration [30] on the reaction $\gamma\gamma \rightarrow K_s^0 K_s^0$ allow one to evaluate the transition $f_2(1800) \rightarrow \gamma\gamma$: Fig. 7 shows the $K_s^0 K_s^0$ spectrum where the peaks are distinctly seen which correspond to the production $f_2(1525)$ and $f_2(1800)$. The description of these peaks in terms of the Breit–Wigner resonances gives us the following relation:

$$\Gamma_{f_2(1800)\rightarrow\gamma\gamma} = (0.10 \pm 0.05) \text{ keV} \cdot \frac{BR(f_2(1525) \rightarrow K\bar{K})}{BR(f_2(1800) \rightarrow K\bar{K})}. \quad (39)$$

Comparing (39) with partial width values shown in Fig. 5c proves that the L3 data agree qualitatively with (38), provided $BR(f_2(1800) \rightarrow K\bar{K}) \sim BR(f_2(1525) \rightarrow K\bar{K})$, that is, the decay channel $f_2(1800) \rightarrow K\bar{K}$ is not small. A rather large magnitude of the branching $f_2(1800) \rightarrow K\bar{K}$ looks natural, because the $f_2(1800)$ and $f_2(1525)$, according to the systematics in the (n, M^2) -plane [25], should belong to the same trajectory, so they both have rather large $s\bar{s}$ component. The fact that, according to (39), partial width of the decay $f_2(1800) \rightarrow \gamma\gamma$ should be greater than $\Gamma_{2^3P_2s\bar{s}\rightarrow\gamma\gamma} \simeq 0.03$ keV may be explained by the (20–30)% admixture of $n\bar{n}$ component in the $f_2(1800)$.

Figure 3d demonstrates form factors for mesons of the $1^3F_2q\bar{q}$ multiplet: the wave functions are defined by (9), while the vertex $T \rightarrow q\bar{q}$ has the form (16). In Fig. 5d partial widths are shown for the transitions $1^3F_2n\bar{n} \rightarrow \gamma\gamma$ and $1^3F_2s\bar{s} \rightarrow \gamma\gamma$ calculated under assumption that masses of these states are of the order of 2000 MeV [25].

4 Conclusion

We have calculated the two-photon decays of tensor mesons, members of the $q\bar{q}$ multiplets $1^3P_2q\bar{q}$, $2^3P_2q\bar{q}$ and $1^3F_2q\bar{q}$.

The main goal was to calculate the decays of mesons of basic multiplet $1^3P_2q\bar{q}$: $a_2(1320)$, $f_2(1270)$ and $f_2(1525)$. All calculated partial widths of radiative decays of these mesons, $a_2(1320) \rightarrow \gamma\gamma$, $f_2(1270) \rightarrow \gamma\gamma$ and $f_2(1525) \rightarrow \gamma\gamma$, are in reasonable agreement with the hypothesis about quark-antiquark structure of tensor mesons. In addition, radial wave functions of $a_2(1320)$, $f_2(1270)$ and $f_2(1525)$ are close to radial wave functions of $a_0(980)$ and $f_0(980)$ found in the study of radiative decays $a_0(980) \rightarrow \gamma\gamma$, $f_0(980) \rightarrow \gamma\gamma$ and $\phi(1020) \rightarrow \gamma\gamma$ [10]. The possibility to describe simultaneously scalar and tensor mesons using approximately equal wave functions may be considered as a strong argument in favour of the fact that all these mesons — tensor $a_2(1320)$, $f_2(1270)$ and $f_2(1525)$ and scalar $a_0(980)$ and $f_0(980)$ — are members of the same P -wave $q\bar{q}$ multiplet.

The mesons of the first radial excitation, according to [25], are $a_2(1660)$, $f_2(1640)$ and $f_2(1800)$. We have calculated partial $\gamma\gamma$ widths for all these mesons. The comparison with data of the L3 Collaboration on the reaction $f_2(1800) \rightarrow \gamma\gamma$ reveals qualitative agreement. However, it should be stressed that calculated values of partial $\gamma\gamma$ widths of mesons belonging to the $2^3P_2q\bar{q}$ multiplet are rather sensitive to details of the wave function of the $q\bar{q}$ system.

We have also calculated the $\gamma\gamma$ width of mesons belonging to the $3^3F_2q\bar{q}$ multiplet. These mesons are located near 2000 MeV [25], and we may expect them to be a target for studying the reactions $\gamma\gamma \rightarrow \text{hadrons}$.

We are grateful to L.G. Dakhno and A.V. Sarantsev for useful discussions. The paper is supported by the RFBR grant n_0 01-02-17861.

Appendix A. Spin structure of the decay amplitude $T \rightarrow \gamma\gamma$

4.1 The completeness of operators $S_{\mu\nu\alpha\beta}^{(H)}$

Here we demonstrate that the convolution of the angular momentum operators for $L = 2$ and $L = 4$ with the helicity operator $S_{\alpha_1\alpha_2, \mu_1\mu_2}^{(2)}$ does not change the amplitude structure given by (1).

The convolution of the helicity $H = 2$ operator with that of $L = 2$ reads:

$$\begin{aligned} X_{\mu_2\beta}^{(2)}(q)S_{\alpha_1\alpha_2, \mu_1\beta}^{(2)}(p, q) &= \tag{A.1} \\ &= \frac{3}{2} \left(q_{\mu_2}^\perp q_\beta^\perp - \frac{1}{3} q_\perp^2 g_{\mu_2\beta}^\perp \right) \left(g_{\mu_1\alpha_1}^\perp g_{\beta\alpha_2}^\perp + g_{\mu_1\alpha_2}^\perp g_{\beta\alpha_1}^\perp - g_{\mu_1\beta}^\perp g_{\alpha_1\alpha_2}^\perp \right) = \\ &= -\frac{q^2}{2} \left(g_{\mu_1\alpha_1}^\perp g_{\mu_2\alpha_2}^\perp + g_{\mu_1\alpha_2}^\perp g_{\mu_2\alpha_1}^\perp - g_{\mu_1\mu_2}^\perp g_{\alpha_1\alpha_2}^\perp \right) = -\frac{q^2}{2} S_{\alpha_1\alpha_2, \mu_1\mu_2}^{(2)}(p, q). \end{aligned}$$

The convolution of the helicity $H = 2$ operator with that of $L = 4$ also gives the term proportional to the $H = 2$ operator:

$$\begin{aligned} X_{\mu_1\mu_2\beta\lambda}^{(4)}(q)S_{\alpha_1\alpha_2, \nu\lambda}^{(2)}(p, q) &= \tag{A.2} \\ &= \frac{35}{8} \left[q_{\mu_1} q_{\mu_2} q_\nu q_\lambda - \frac{q^2}{7} \left(g_{\mu_1\mu_2}^\perp q_\nu q_\lambda + g_{\mu_1\nu}^\perp q_{\mu_2} q_\lambda + g_{\mu_2\nu}^\perp q_{\mu_1} q_\lambda + g_{\nu\lambda}^\perp q_{\mu_1} q_{\mu_2} \right) - \right. \\ &\left. - \frac{q^4}{35} \left(g_{\mu_1\mu_2}^\perp g_{\nu\lambda}^\perp + g_{\mu_1\nu}^\perp g_{\mu_2\lambda}^\perp + g_{\mu_1\lambda}^\perp g_{\mu_2\nu}^\perp \right) \right] \left(g_{\nu\alpha_1}^\perp g_{\lambda\alpha_2}^\perp + g_{\nu\alpha_2}^\perp g_{\lambda\alpha_1}^\perp - g_{\nu\lambda}^\perp g_{\alpha_1\alpha_2}^\perp \right) = \end{aligned}$$

$$= \frac{q^4}{4} \left(g_{\mu_1 \alpha_1}^{\perp \perp} g_{\mu_2 \alpha_2}^{\perp \perp} + g_{\mu_1 \alpha_2}^{\perp \perp} g_{\mu_2 \alpha_1}^{\perp \perp} - g_{\mu_1 \mu_2}^{\perp \perp} g_{\alpha_1 \alpha_2}^{\perp \perp} \right) = \frac{q^4}{4} S_{\alpha_1 \alpha_2, \mu_1 \mu_2}^{(2)}(p, q).$$

So, we see that the both convolutions, the $H = 2$ operator with $L = 2$ and $L = 4$, give the terms proportional to $S_{\alpha_1 \alpha_2, \mu_1 \mu_2}^{(2)}(p, q)$.

4.2 The operators $S_{\mu\nu\alpha\beta}^{(H)}$ and standard helicity technique

To demonstrate the connection of the introduced operators with standard helicity technique, consider as an example the transition $\gamma\gamma \rightarrow 2^{++} - \text{resonance} \rightarrow \pi^0\pi^0$. Using the momenta q_1, q_2 for photons and k_1, k_2 for mesons, one has for relative momenta and photon polarization vectors

$$q = \frac{1}{2}(q_1 - q_2) = (0, 0, 0, q_z), \quad k = \frac{1}{2}(k_1 - k_2) = (0, k_x, k_y, k_z), \quad (A.3)$$

$$\epsilon = (0, \epsilon_x, \epsilon_y, 0) = (0, \cos \phi, \sin \phi, 0).$$

In the helicity basis

$$\epsilon = (0, \epsilon_+, \epsilon_-, 0), \quad (A.4)$$

$$\epsilon_+ = -\frac{1}{\sqrt{2}}(\epsilon_x + i\epsilon_y), \quad \epsilon_- = \frac{1}{\sqrt{2}}(\epsilon_x - i\epsilon_y)$$

The spin-dependent part of the amplitude with $H = 0$ reads:

$$\epsilon_{\alpha}^{(1)} \epsilon_{\beta}^{(2)} S_{\alpha\beta}^{(0)} X_{\mu\nu}^{(2)}(q) X_{\mu\nu}^{(2)}(k) = \frac{9}{4} q^2 k^2 (\cos^2 \theta - \frac{1}{3}) (\epsilon_+^{(1)} \epsilon_+^{(2)} + \epsilon_-^{(1)} \epsilon_-^{(2)}). \quad (A.5)$$

For $H = 2$ one has

$$\epsilon_{\alpha}^{(1)} \epsilon_{\beta}^{(2)} S_{\alpha\beta\mu\nu}^{(2)} X_{\mu\nu}^{(2)}(k). \quad (A.6)$$

Different components are written as follows:

$$\epsilon_+^{(1)} \epsilon_+^{(2)} S_{++\mu\nu}^{(2)} X_{\mu\nu}^{(2)}(k) = 0, \quad (A.7)$$

$$\epsilon_+^{(1)} \epsilon_-^{(2)} S_{+-\mu\nu}^{(2)} X_{\mu\nu}^{(2)}(k) = \frac{3}{2} k^2 \sin^2 \theta \left(1 + 2i \sin \phi e^{i\phi} \right),$$

$$\begin{aligned}\epsilon_-^{(1)} \epsilon_+^{(2)} S_{-\mu\nu}^{(2)} X_{\mu\nu}^{(2)}(k) &= \frac{3}{2} k^2 \sin^2 \theta \left(1 - 2i \sin \phi e^{-i\phi}\right), \\ \epsilon_-^{(1)} \epsilon_-^{(2)} S_{-\mu\nu}^{(2)} X_{\mu\nu}^{(2)}(k) &= 0.\end{aligned}$$

4.3 Operators $S_{\mu\nu\alpha\beta}^{(H)}$ and analytical properties of vertex function

The operators $S_{\mu\nu\alpha\beta}^{(H)}$ are expressed through metric tensors $g_{\alpha\beta}^{\perp\perp}$ which work in the space perpendicular to the reaction plane $T \rightarrow \gamma\gamma$. This metric tensor has the structure as follows:

$$g_{\alpha\beta}^{\perp\perp} = g_{\alpha\beta} - p_\alpha p_\beta / m_T^2 + 4q_\alpha q_\beta / m_T^2. \quad A.8$$

The presence of factors $1/m_T^2$ may evoke the question about the behaviour of the form factor amplitude at $m_T^2 = 0$. Of course, this is a far remote point for the reactions under consideration (the lowest tensor resonance is at $m_T \simeq 1600$ GeV²). Still, this problem sounds principal, so consider it in details.

When treating the reaction "composite system $\rightarrow \gamma\gamma$ " one should distinguish it from the transition "constituents $\rightarrow \gamma\gamma$ ", in this case $q\bar{q} \rightarrow \gamma\gamma$. These processes though related to each other are different: the amplitude for the process "composite system $\rightarrow \gamma\gamma$ " (or $T \rightarrow \gamma\gamma$) is determined by the residue in the amplitude pole $q\bar{q} \rightarrow \gamma\gamma$ at $s = m_T^2$, where s is the invariant energy squared of the $q\bar{q}$ system. Both amplitudes should satisfy the requirement of gauge invariance (this requirement for the transition $T \rightarrow \gamma\gamma$ is imposed by the operators $S_{\mu\nu\alpha\beta}^{(H)}$), but they have different analytical properties. In particular, the threshold theorems appropriate for $q\bar{q} \rightarrow \gamma\gamma$ do not take place in the vertex function, i.e. for the residue in the pole $s = m_T^2$ the threshold theorems

are realised by the interplay of pole and non-pole terms. Due to this fact we must keep the mass of the tensor meson m_T^2 in Eq. (A.8) as fixed value.

The problem of interrelation of gauge invariance and analyticity in the spectral integration technique has been discussed in detail in [21, 23] for the transitions $q\bar{q} \rightarrow \gamma q\bar{q}$, $NN \rightarrow \gamma NN$, $NN\gamma \rightarrow NN\gamma$ and corresponding vertex functions describing composite systems (mesons and deuteron).

An opposite point of view according to which the threshold theorems should work for vertex functions was outspoken in [31].

Appendix B. Spin factors for pure $q\bar{q}(L = 1)$ and $q\bar{q}(L = 3)$ states

At small Q^2 the spin factor $S_{L=1}^{(H=0)}(P^2 = s, P'^2 = s', -Q^2)$ for pure ($L = 1$)-state reads:

$$\begin{aligned}
S_{L=1}^{(0)}(s, s', -Q^2) &= \tag{B.1} \\
&= \frac{32\Sigma^2 Q^4}{(\Delta^2 + 4\Sigma Q^2)^2} \left[2m^2 (4m^2 - \Sigma) - \frac{m(4m^2 - \Sigma)^2}{2m + \sqrt{\Sigma}} \right] + \\
&+ \frac{4\Sigma Q^2 \Delta^2}{(\Delta^2 + 4\Sigma Q^2)^2} \left[(32m^4 + 8m^2\Sigma - 3\Sigma^2) - \frac{4m(16m^4 - \Sigma^2)}{2m + \sqrt{\Sigma}} \right] + \\
&+ \frac{4m^2 \Delta^4}{(\Delta^2 + 4\Sigma Q^2)^2} \left[(4m^2 + 3\Sigma) - \frac{4m(2m^2 + \Sigma)}{2m + \sqrt{\Sigma}} \right]
\end{aligned}$$

Recall that we use the notations $\Sigma = (s + s')/2$ and $\Delta = s - s'$.

For $H = 2$ one has:

$$\begin{aligned}
S_{L=1}^{(2)}(s, s', -Q^2) &= \tag{B.2} \\
&= \frac{8\Sigma^2 Q^4}{(\Delta^2 + 4\Sigma Q^2)^2} \left[(-16m^4 + \Sigma^2) + \frac{2m(4m^2 - \Sigma)^2}{2m + \sqrt{\Sigma}} \right] +
\end{aligned}$$

$$\begin{aligned}
& + \frac{4\Sigma Q^2 \Delta^2}{(\Delta^2 + 4\Sigma Q^2)^2} \left[(-16m^4 - 4m^2\Sigma + \Sigma^2) + \frac{8m^3(4m^2 - \Sigma)}{2m + \sqrt{\Sigma}} \right] + \\
& + \frac{4m^2 \Delta^4}{(\Delta^2 + 4\Sigma Q^2)^2} \left[(-2m^2 - \Sigma) + \frac{4m^3}{2m + \sqrt{\Sigma}} \right].
\end{aligned}$$

Correspondingly, the spin factors $S_{L=3}^{(H)}(s, s', -Q^2)$ for pure ($L = 3$)-state are as follows:

$$\begin{aligned}
& S_{L=3}^{(0)}(s, s', -Q^2) = \tag{B.3} \\
& = \frac{48\Sigma^2 Q^4}{5(\Delta^2 + 4\Sigma Q^2)^2} \left[2m^2(4m^2 - \Sigma)^2 - \frac{m(4m^2 - \Sigma)^3}{2m + \sqrt{\Sigma}} \right] + \\
& + \frac{12\Sigma Q^2 \Delta^2}{5(\Delta^2 + 4\Sigma Q^2)^2} \left[(16m^4 + 4m^2\Sigma + \Sigma)(4m^2 - \Sigma) - \frac{2m(4m^2 + \Sigma)(4m^2 - \Sigma)^2}{2m + \sqrt{\Sigma}} \right] + \\
& + \frac{12m^2 \Delta^4}{5(\Delta^2 + 4\Sigma Q^2)^2} \left[(8m^4 + 4m^2\Sigma + \Sigma^2) - \frac{2m(4m^2 - \Sigma)(2m^2 + \Sigma)}{2m + \sqrt{\Sigma}} \right],
\end{aligned}$$

and

$$\begin{aligned}
& S_{L=3}^{(2)}(s, s', -Q^2) = \tag{B.4} \\
& = \frac{4\Sigma^2 Q^4}{5(\Delta^2 + 4\Sigma Q^2)^2} \left[(-6m^2 + \Sigma)(4m^2 - \Sigma)^2 + \frac{3m(4m^2 - \Sigma)^3}{2m + \sqrt{\Sigma}} \right] + \\
& + \frac{2\Sigma Q^2 \Delta^2}{5(\Delta^2 + 4\Sigma Q^2)^2} \left[(-24m^4 + 4m^2\Sigma - \Sigma^2)(4m^2 - \Sigma) + \frac{12m^3(4m^2 - \Sigma)^2}{2m + \sqrt{\Sigma}} \right] + \\
& + \frac{2m^2 \Delta^4}{5(\Delta^2 + 4\Sigma Q^2)^2} \left[(-12m^4 + 2m^2\Sigma - \Sigma^2) + \frac{6m^3(4m^2 - \Sigma)}{2m + \sqrt{\Sigma}} \right].
\end{aligned}$$

Appendix C. Transition form factors $F_{T(L) \rightarrow \gamma\gamma}^{(H)}(0, 0)$

Spectral integral for the form factor $F_{T(L) \rightarrow \gamma\gamma}^{(H)}(0, 0)$ with pure ($L = 1$) or ($L = 3$) wave in the vertex $T \rightarrow q\bar{q}$ reads as follows:

$$F_{T(L) \rightarrow \gamma\gamma}^{(H)}(0, 0) = \frac{Z^{(q\bar{q})} \sqrt{N_c}}{16\pi} \int_{4m^2}^{\infty} \frac{ds}{\pi} \psi_T(s) \psi_\gamma(s) I_L^{(H)}(s), \tag{C.1}$$

where for ($L = 1$) one has

$$I_{L=1}^{(0)}(s) = -2\sqrt{s(s-4m^2)}(12m^2+3) + 4m^2(4m^2+3s) \ln \frac{s + \sqrt{s(s-4m^2)}}{s - \sqrt{s(s-4m^2)}} +$$

$$+ \frac{16m^3}{2m + \sqrt{s}} \left[3\sqrt{s(s-4m^2)} - (2m^2 + s) \ln \frac{s + \sqrt{s(s-4m^2)}}{s - \sqrt{s(s-4m^2)}} \right] \quad (C.2)$$

and

$$I_{L=1}^{(2)}(s) = \frac{4\sqrt{s(s-4m^2)}}{3}(5m^2+s) - 4m^2(2m^2+s) \ln \frac{s + \sqrt{s(s-4m^2)}}{s - \sqrt{s(s-4m^2)}} +$$

$$+ \frac{4m}{2m + \sqrt{s}} \left[-\frac{\sqrt{s(s-4m^2)}}{3}(10m^2-s) + 4m^4 \ln \frac{s + \sqrt{s(s-4m^2)}}{s - \sqrt{s(s-4m^2)}} \right]. \quad (C.3)$$

Analogously, for the $q\bar{q}(L=3)$ -wave ($1^3F_2q\bar{q}$ multiplet), we have

$$I_{L=3}^{(0)}(s) = -\frac{2\sqrt{s(s-4m^2)}}{5}(72m^4+8m^2s+s^2) + \quad (C.4)$$

$$+ \frac{12}{5}m^2(8m^4+4m^2s+s^2) \ln \frac{s + \sqrt{s(s-4m^2)}}{s - \sqrt{s(s-4m^2)}} +$$

$$+ \frac{24m^3(s-4m^2)}{5(2m + \sqrt{s})} \left[-3\sqrt{s(s-4m^2)} + (2m^2+s) \ln \frac{s + \sqrt{s(s-4m^2)}}{s - \sqrt{s(s-4m^2)}} \right]$$

and

$$I_{L=3}^{(2)}(s) = \frac{2\sqrt{s(s-4m^2)}}{15}(30m^4-4m^2s+s^2) - \quad (C.5)$$

$$- \frac{2}{5}m^2(12m^4-2m^2s+s^2) \ln \frac{s + \sqrt{s(s-4m^2)}}{s - \sqrt{s(s-4m^2)}} +$$

$$+ \frac{m(s-4m^2)}{5(2m + \sqrt{s})} \left[\sqrt{s(s-4m^2)}(10m^2-s) - 12m^4 \ln \frac{s + \sqrt{s(s-4m^2)}}{s - \sqrt{s(s-4m^2)}} \right].$$

References

- [1] E. Klempt, hep-ex/0101031 (2001).
- [2] L. Montanet, Nucl. Phys. Proc. Suppl. **86**, 381 (2000).
- [3] R. Ricken, M. Koll, D. Merten, B.C. Metsch, and H.R. Petry, Eur. Phys. J. A **9**, 221 (2000).
- [4] V. V. Anisovich, Physics-Uspekhi, **41** 419 (1998).
- [5] V. V. Anisovich, Yu. D. Prokoshkin, and A. V. Sarantsev, Phys. Lett. B **389**, 388 (1996);
V.V. Anisovich, A.A. Kondashov, Yu.D. Prokoshkin, S.A. Sadovsky, A.V. Sarantsev, Yad. Fiz. **60**, 1489 (2000) [Physics of Atomic Nuclei, **60**, 1410 (2000)].
- [6] A. V. Anisovich and A. V. Sarantsev, Phys. Lett. B **413**, 137 (1997).
- [7] V. V. Anisovich, D. V. Bugg, and A. V. Sarantsev, Phys. Lett. B **437**, 209 (1998); Yad. Fiz. **62**, 1322 (1999) [Phys. Atom. Nucl. **62**, 1247 (1999)].
- [8] V.V. Anisovich, L. Montanet, and V.A. Nikonov, Phys. Lett. B **480**, 19 (2000).
- [9] A. V. Anisovich, V. V. Anisovich, D. V. Bugg, and V.A. Nikonov, Phys. Lett. B **456**, 80 (1999).
- [10] A.V. Anisovich, V. V. Anisovich, V.N. Markov, and V.A. Nikonov, *Radiative decays and quark content of $f_0(980)$ and $\phi(1020)$* , Yad. Fiz., in press.

- [11] S. Spanier and N.A. Törnqvist, Eur. Phys. J. C **15**, 437 (2000).
- [12] V.V. Anisovich, A.A. Anselm, Ya.I. Azimov, G.S. Danilov, and I.T. Dyatlov, Phys. Lett. **16**, 194 (1965).
- [13] W.E. Tiring, Phys. Lett. **16**, 335 (1965).
- [14] L.D. Solovjev, Phys. Lett. **16**, 345 (1965).
- [15] C. Becchi and G. Morpurgo, Phys. Rev. **140**, 687 (1965).
- [16] R. R. Akhmetshin *et al.*, CMD-2 Collab., Phys. Lett. B **462**, 371 (1999);
462, 380 (1999);
M. N. Achasov *et al.*, SND Collab., Phys. Lett. B **485**, 349 (2000).
- [17] M. Boglione and M. R. Pennington, Eur. Phys. J. C **9**, 11 (1999).
- [18] V. V. Anisovich, V. A. Nikonov, and A. V. Sarantsev, *Quark-gluonium content of the scalat-isoscalar states $f_0(980)$, $f_0(1300)$, $f_0(1500)$, $f_0(1750)$, $f_0(1420_{-70}^{+150})$ from hadronic decays*, Yad. Fiz., in press; hep-ph/0108188.
- [19] E. Borchini and R. Gatto, Phys. Lett. **14**, 352 (1965).
- [20] V.V. Anisovich, A.A. Anselm, Ya.I. Azimov, G.S. Danilov, and I.T. Dyatlov, Pis'ma ZETF **2**, 109 (1965).
- [21] V. V. Anisovich, D. I. Melikhov, and V. A. Nikonov, Phys. Rev. D **55**, 2918 (1997); **52**, 5295 (1995).
- [22] Yu. D. Prokoshkin *et al.*, Physics-Doklady **342**, 473 (1995);
D. Alde *et al.*, Z. Phys. C **66**, 375 (1995).

- [23] V. V. Anisovich, M. N. Kobrinsky, D. I. Melikhov, and A. V. Sarantsev, Nucl. Phys. A **544**, 747 (1992); Yad. Fiz. **55**, 1773 (1992).
- [24] V.V. Anisovich, *Elements of scattering theory*, Chapter V, in: "Hadron Spectroscopy and Confinement Problem", Ed. D.V. Bugg, NATO ASI Series, Physics (Plenum Press, New York and London, (1996)),Vol. 353.
- [25] A.V. Anisovich, V.V. Anisovich, A.V. Sarantsev, Phys. Rev. D **62**:051502(R), (2000).
- [26] H. Albrecht *et al.*, ARGUS Collab.Z. Phys. C **74**, 469 (1997).
- [27] M. Acciarri *et al.*, L3 Collab., Phys. Lett. B **413**, 147 (1997).
- [28] H. Albrecht *et al.*,ARGUS Collab., Z. Phys. C **48**, 183 (1990).
- [29] PDG Group, D. E. Groom *et al.*, Eur. Phys. J. C **15**, 1 (2000).
- [30] V.A. Schegelsky, "*Resonance production in two-photon collisions at LEP (Experiment L3)*", 9 th International Conference on Hadron Spectroscopy, HADRON-2001, August 27-September 1, Protvino, Russia.
- [31] N.N. Achasov, hep-ph/0110059.

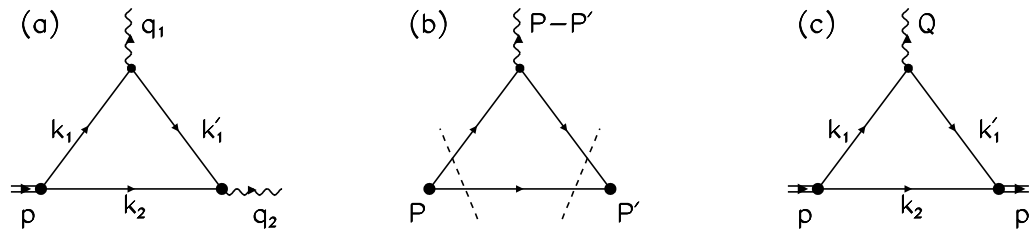


Figure 1: (a) Triangle diagram for the transition form factor $T \rightarrow \gamma(q_1^2)\gamma(q_2^2)$; (b) diagram for the double spectral representation over $P^2 = s$ and $P'^2 = s'$; the intermediate-state particles are mass-on-shell, the cuttings of the diagram are shown by dashed lines; (c) triangle diagram for the meson charge form factor.

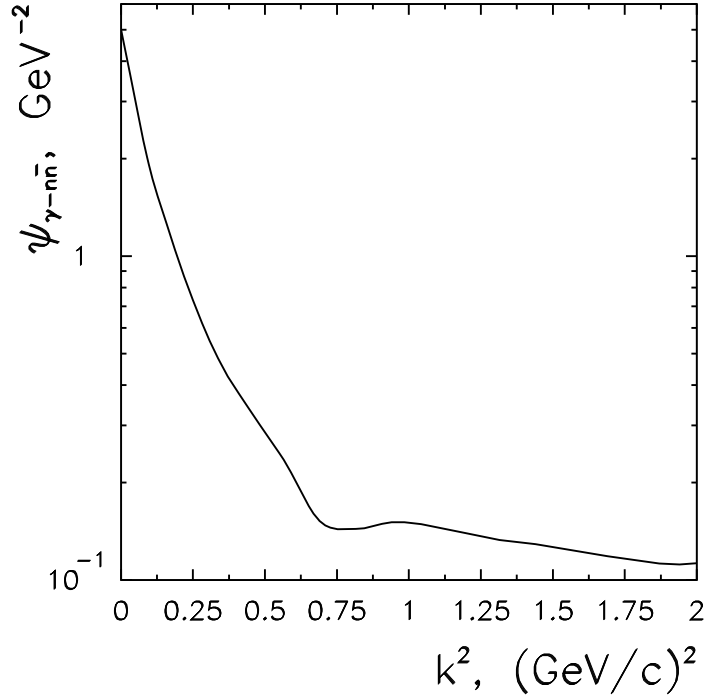


Figure 2: Photon wave function for non-strange quarks, $\psi_{\gamma \rightarrow n\bar{n}}(k^2) = g_\gamma(k^2)/(k^2 + m^2)$, where $k^2 = s/4 - m^2$; the wave function for the $s\bar{s}$ component is equal to $\psi_{\gamma \rightarrow s\bar{s}}(k^2) = g_\gamma(k^2)/(k^2 + m_s^2)$ where m_s is the constituent s -quark mass.

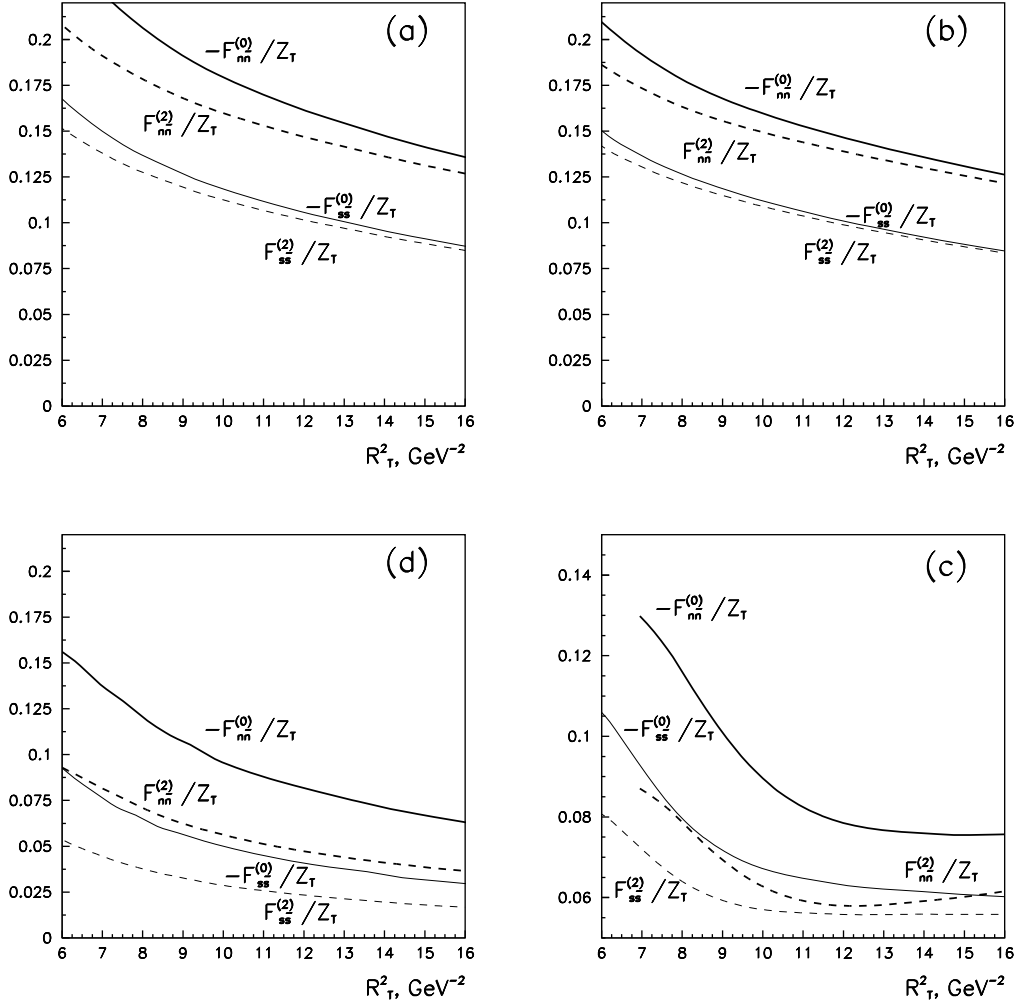


Figure 3: Transition form factors $T \rightarrow \gamma\gamma$ (see (17) or (24)) for the non-strange ($n\bar{n}$) and strange ($s\bar{s}$) quarks versus mean tensor meson radius squared, R_T^2 . (a) $F_{q\bar{q}}^{(H)}(0,0)$ for $1^3P_2q\bar{q}$ state with minimal vertex, Eqs. (9) and (12); (b) the same as Fig. 3a but for the vertex determined by (15); (c) $F_{q\bar{q}}^{(H)}(0,0)$ for $2^3P_2q\bar{q}$ state with the vertex given by (10) and (12); (d) $F_{q\bar{q}}^{(H)}(0,0)$ for $1^3F_2q\bar{q}$ state with vertex given by (9) and (16).

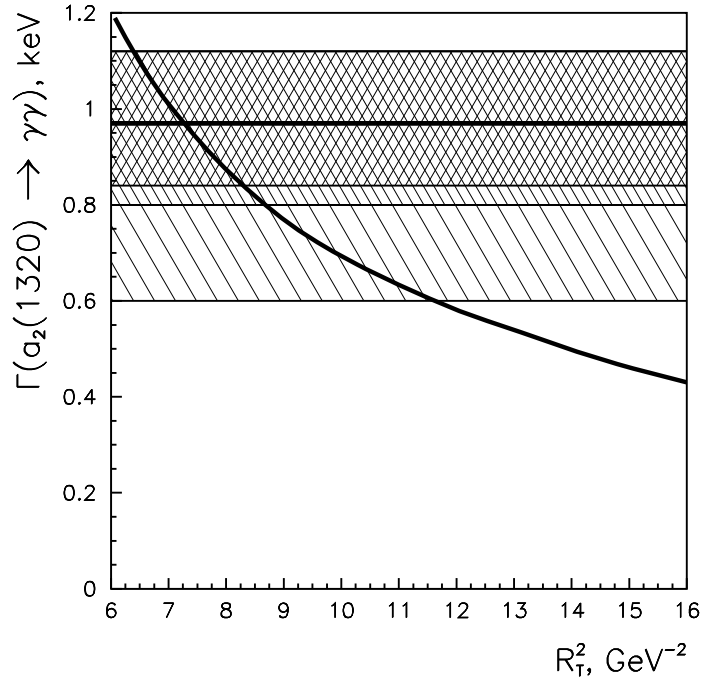


Figure 4: Partial width $\Gamma(a_2(1320) \rightarrow \gamma\gamma)$ (thick solid line) versus the data (hatched areas, see section 3.3) as a function of the mean meson radius squared, R_T^2 , for the vertex determined by Eqs. (9) and (12).

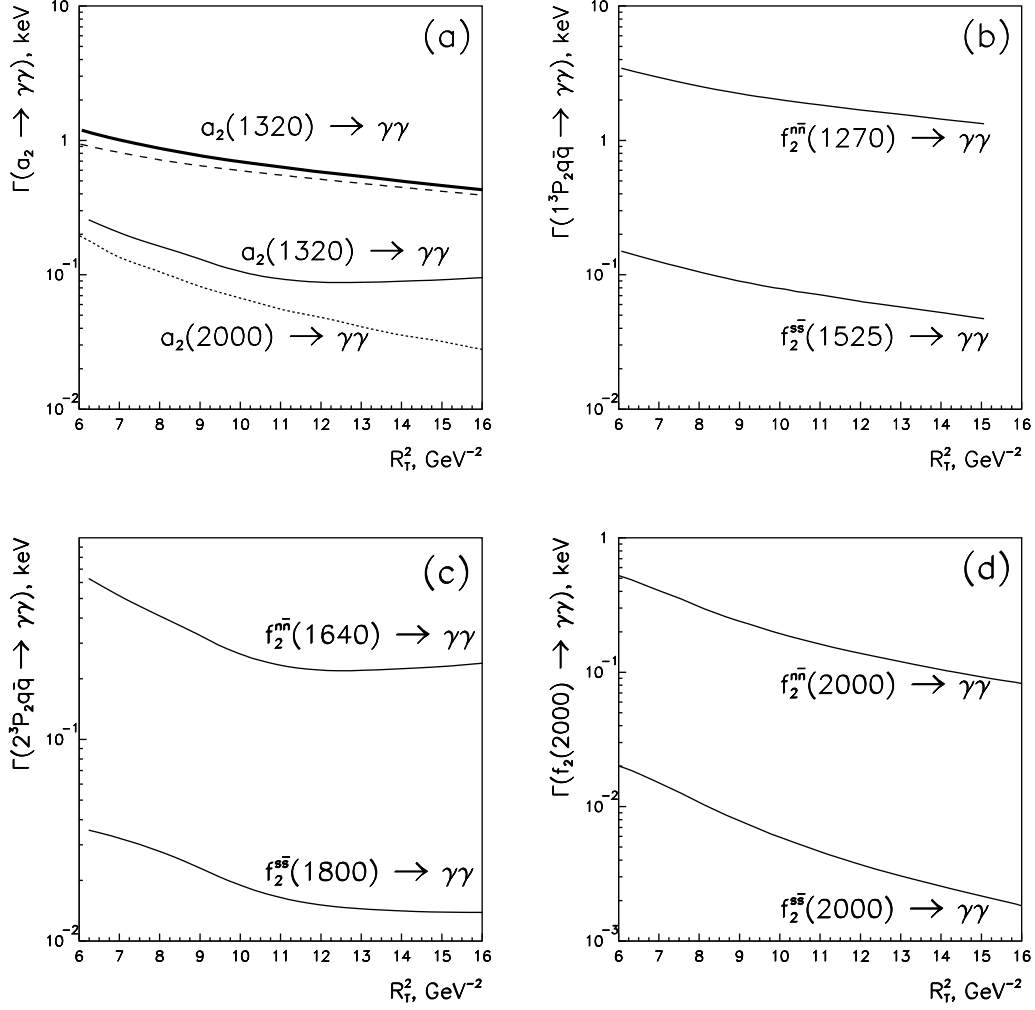


Figure 5: Partial widths for a_2 and f_2 mesons versus mean tensor-meson radius squared, R_T^2 . (a) Thick solid line: $\Gamma(a_2(1320) \rightarrow \gamma\gamma)$ for the vertex given by (9) and (12); dashed line: $\Gamma(a_2(1320) \rightarrow \gamma\gamma)$ for the vertex given by (9) and (15); dotted line: $\Gamma(a_2(\sim 2000) \rightarrow \gamma\gamma)$ for the vertex given by (9) and (16); thin solid line: $\Gamma(a_2(1660) \rightarrow \gamma\gamma)$ for the vertex given by (10) and (12). (b) Partial widths for isoscalar mesons of the basic $1^3P_3q\bar{q}$ nonet: for $f_2(1525)$ meson supposing it is either pure $s\bar{s}$ state and for $f_2(1270)$ under assumption it is pure $n\bar{n}$. (c) Partial width for $f_2(1800)$ meson supposing it is the pure $2^3P_2s\bar{s}$ state and for $f_2(1640)$ considered³⁵ as a pure $2^3P_2n\bar{n}$ state. (d) Partial widths for $1^3F_2s\bar{s}$ and $1^3F_2n\bar{n}$ states with mass ~ 2000 MeV.

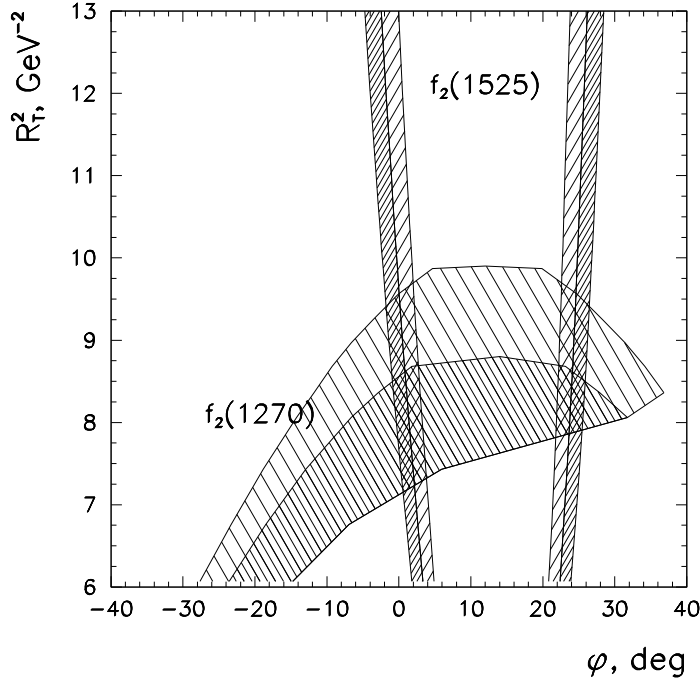


Figure 6: The (R_T^2, φ) -plot, where φ is mixing angle for the flavour components $f_2(1270) = n\bar{n} \cos \varphi + s\bar{s} \sin \varphi$ and $f_2(1525) = -n\bar{n} \sin \varphi + s\bar{s} \cos \varphi$, with hatched areas which show the regions allowed by data for decays $f_2(1270) \rightarrow \gamma\gamma$ and $f_2(1525) \rightarrow \gamma\gamma$.

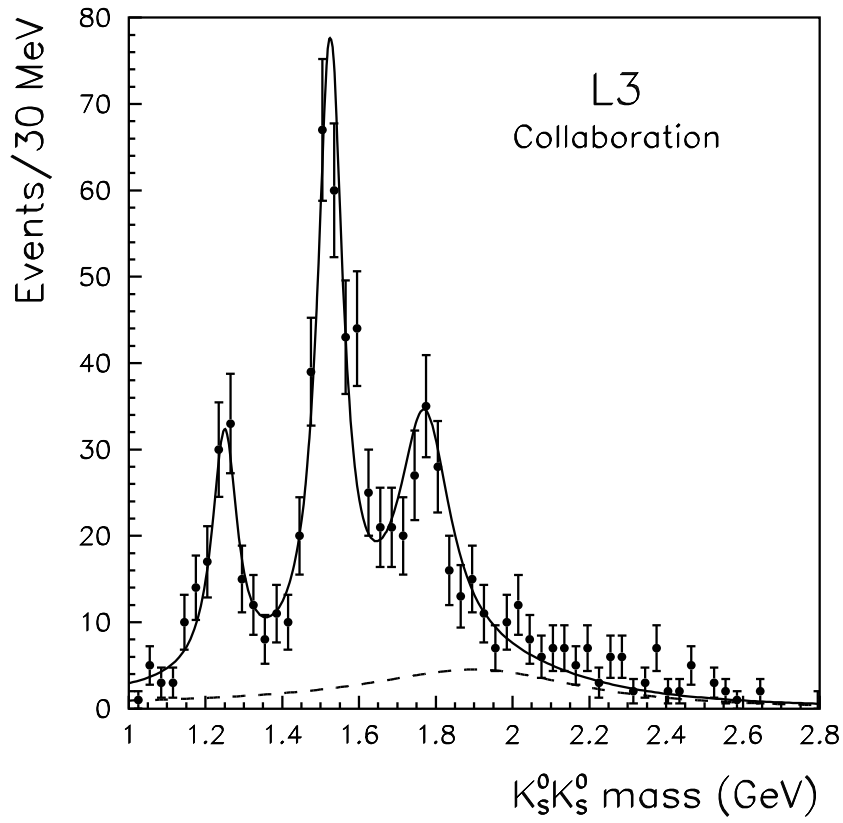


Figure 7: The $K_s^0 K_s^0$ mass spectrum in $\gamma\gamma \rightarrow K_s^0 K_s^0$ [30] with production $f_2(1525)$ and $f_2(1800)$.